Dalton Transactions

ROYAL SOCIETY OF CHEMISTRY

COMMUNICATION

View Article Online
View Journal | View Issue

Cite this: *Dalton Trans.*, 2020, **49**, 1726

Received 3rd January 2020,
Accepted 9th January 2020

DOI: 10.1039/d0dt00024h

rsc.li/dalton

Diverse structure and reactivity of pentamethylcyclopentadienyl antimony(III) cations†

Omar Coughlin, [a] Tobias Krämer [b] and Sophie L. Benjamin *[a]

The pentamethylcyclopentadienyl (Cp*) antimony(III) cations $[Cp^*_2Sb][B(C_6F_5)_4]$, $[Cp_2{}^*Sb][OTf]$, $[Cp^*SbCl][B(C_6F_5)_4]$ and $[Cp^*Sb][OTf]_2$ have been isolated and structurally characterised. $[Cp^*SbCl]^+$ forms dimers in the solid state *via* an intermolecular Sb–Cl interaction. Initial screening shows that $[Cp^*SbCl][B(C_6F_5)_4]$ is significantly Lewis acidic and can catalyse the dimerisation of 1,1-diphenylethylene; $[Cp_2{}^*Sb][B(C_6F_5)_4]$ exhibits negligible Lewis acidity. Highly unstable $[Cp^*SbF][B(C_6F_5)_4]$ could not be isolated, but stabilisation with the IMes ligand allowed isolation of $[Cp^*SbF(IMes)][B(C_6F_5)_4]$. Fluorodechlorination of CH_2Cl_2 and $PhCCl_3$ was observed in the presence of crude $[Cp^*SbF][B(C_6F_5)_4]$ in solution. A computational mechanistic investigation suggests that the latter proceeds *via* a carbocation intermediate.

There is an increasing recognition that main group reagents have the potential to replace transition metals in synthetic applications, giving advantages in cost and broadening the scope of available reactivity.[1–3] Organo-group 15 cations have recently been identified as potent and versatile Lewis acid catalysts. The majority of attention has focused on electrophilic P(v) cations as catalysts for a varied and growing range of transformations, including hydrosilylation, hydrodefluorination, and arylation of benzyl fluorides.[4–6] Lewis acid catalysis has also been demonstrated in several preliminary studies with Sb(v) cations.[7–9] A recent investigation into the use of pnictogen, chalcogen and halogen bonding for anion binding catalysis demonstrated that neutral Sb(III) centres were by far the most active compared with P, As, Se, Te, Br and I analogues, giving a strong imperative for the further study of this behaviour.[10] Introduction of halogen substituents at Sb has been shown to increase the strength of pnictogen bonding,[11] and acceptor behaviour could be further enhanced by the introduction of a positive charge. Despite the renewed interest in Sb(v) cations, little investigation has been made into the reactivity of Sb(III) cations. Reported examples commonly feature stabilisation from Lewis bases.[12–14] We hypothesised that inclusion of Cp* ligands would allow the isolation of Sb(III) cations without the need for additional stabilisation, yielding significant Lewis acidity at the Sb centre and making them ideal targets in the search for novel, tuneable main group reagents.

Metallocenes are ubiquitous in transition metal chemistry. First discovered serendipitously in 1951,[15] ferrocene and its derivatives now find diverse applications as catalysts,[16] ligand scaffolds[17,18] and redox reagents.[19] Main group 'metallocenes', or more broadly main group complexes with cyclopentadienyl (Cp) or substituted Cp′ ligands, have more variation in metal–ligand binding modes, giving rise to greater structural diversity than their transition metal counterparts.[20–22] Intermolecular interactions are prevalent, leading to the observation of dimers, oligomers and polymers in the solid state.[20] The absence of available d-orbitals for bonding means that M–Cp′ bonds are often fairly labile and, unlike traditional metallocenes, they show significant reactivity at both the metal centre and the ligands. While there has been considerable research into the properties of s-block and group 14 metallocenes, reports of group 15 metallocenes are relatively uncommon, and until recently have been limited to synthetic and structural investigations (Fig. 1).[23–25] Very recently the dicationic $[Cp^*M][B(C_6F_5)_4]_2$ (M = P, As) and $[Cp^*B(Mes)][B(C_6F_5)_4]_2$ have been reported, all of which are potent Lewis acids.[26–28]

Equimolar addition of $[(Et_3Si)C_7H_8][B(C_6F_5)_4]$ to Cp^*_2SbCl in toluene led to the formation of the dark red sandwich 'sti-

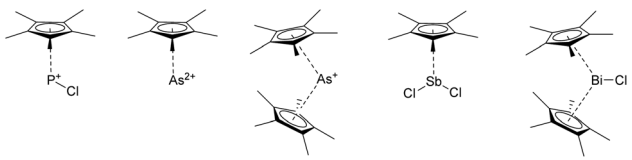

Fig. 1 Examples of neutral, monocationic and dicationic group 15 metallocenes reported in the literature.[25–27,29]

[a]*Department of Chemistry and Forensics, Nottingham Trent University, Clifton Lane, NG11 8NS Nottingham, UK. E-mail: sophie.benjamin@ntu.ac.uk*
[b]*Department of Chemistry, Maynooth University, Maynooth, Co Kildare, Ireland*

†Electronic supplementary information (ESI) available. CCDC 1967954–1967959. For ESI and crystallographic data in CIF or other electronic format see DOI: 10.1039/d0dt00024h

bocenium' complex $[Cp^*_2Sb][B(C_6F_5)_4]$ (**1**) (Scheme 1). The X-ray structure of **1** demonstrates that the Cp* ligands coordinate to Sb with η^4/η^3 hapticity in the solid state (Fig. 2a). The sandwich is somewhat bent with a $Cp^*_{centroid}$–Sb–$Cp^*_{centroid}$ angle of 158.08°. The lone pair in group 15 metallocenes tend to be lower in energy and of greater s-character than other organopnictogen(III) compounds; deviation from linear structures in main group metallocenes are prevalent and has been attributed to a combination of through space coupling effect and some degree of s/p mixing for lone pair orbitals.[22,30] Two aluminate salts of the same cation, $[Cp^*_2Sb][AlX_4]$ (X = Cl, I), have previously been reported as well as with the $[BF_4]^-$ salt.[23,25,31] Unlike **1**, reported structures contain Sb–anion interactions, with somewhat different bond lengths and angles in the cation compared to **1** (Table 7, ESI†). Thus **1** is the first example of a truly 'naked' stibocenium cation to be structurally characterised. To probe the influence of electronic *vs.* packing effects on the structure, $[Cp^*_2Sb][OTf]$ (**1a**) was also synthesised and structurally characterised. **1a** was also found to have no Sb–anion interactions, providing a direct comparison for **1** with a unique packing environment. Structural parameters in the cationic $[Cp^*_2Sb]^+$ fragment in **1** and **1a** were remarkably similar, suggesting that electronic effects are predominant in determining the structural parameters of $[Cp^*_2Sb]^+$ in the solid state.

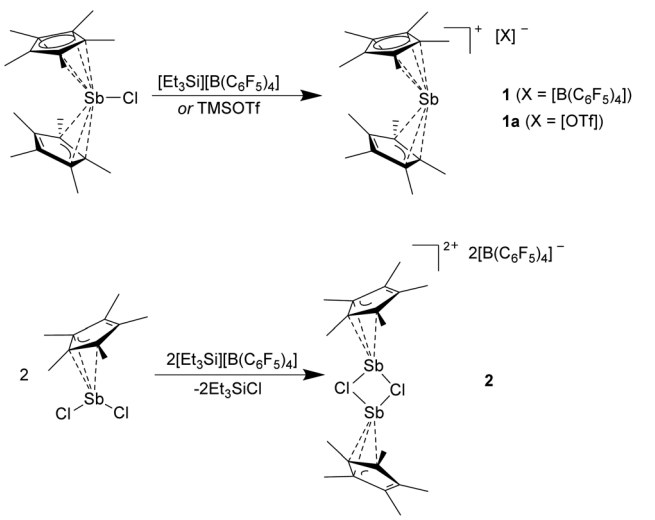

Scheme 1 Synthesis of **1** (top) and **2** (bottom). Conditions: Toluene, room temperature (**1** and **2**), dichloromethane, room temperature (**1a**).

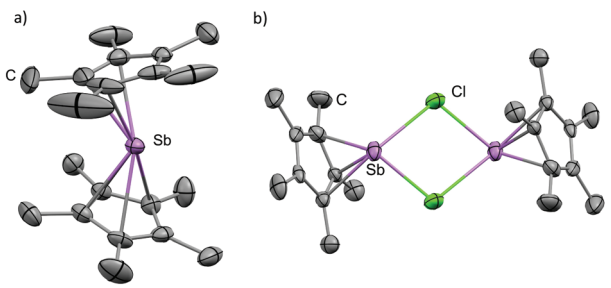

Fig. 2 (a) Solid state structure of the cation in **1**. Ellipsoids are shown at 50% probability. Hydrogen atoms are omitted for clarity. The hapticity of both Cp* rings is η^4/η^3. (b) Solid structure of the cation in **2**. Ellipsoids are shown at 50% probability. Hydrogen atoms are omitted for clarity. The hapticity of the Cp* ring is η^3.

Equimolar addition of $[(Et_3Si)C_7H_8][B(C_6F_5)_4]$ to Cp^*SbCl_2 in toluene yielded light yellow crystals of the half-sandwich complex $[Cp^*SbCl][B(C_6F_5)_4]$ (**2**) (Scheme 1). The $[Cp^*SbCl]^+$ cation forms dimers in the solid state (Fig. 2b) through an intermolecular Sb–Cl interaction (2.553(2) Å), indicating significant Lewis acidity at the Sb centre. The Cp* ligand adopts η^3 hapticity, with a $Cp^*_{centroid}$–Sb distance of 2.142 Å and a $Cp^*_{centroid}$–Sb–Cl_{intra} angle of 122.23°. This deviation from trigonal pyramidal geometry suggests that the formal lone pair on the Sb is isotropic, as is commonly observed in main group metallocenes.[20] If left to stand over a period of days in aromatic solvent, reaction solutions of **2** were found to decompose into a mixture of products, including a significant quantity of **1**. This type of substituent scrambling is common in organoantimony chemistry and demonstrates the lability of the Sb–Cp* bonding.

With **1** and **2** in hand, we sought to investigate their coordination chemistry and reactivity. The ^{31}P NMR spectrum obtained from an equimolar solution of **2** and Et_3PO in CD_2Cl_2 shows a signal at 75 ppm (*vs.* 52 ppm for free Et_3PO). The ^1H NMR spectrum obtained from an equimolar solution of **2** and pyridine in CD_2Cl_2 also suggests the formation of an adduct, indicated by a strong shift downfield of the pyridine protons and a weak shift upfield on the Cp^*_{methyl} protons. The same experiment with **1** gave a ^1H NMR spectrum which was equivalent to the sum of the spectra of **1** and pyridine, suggesting no adduct formation.

Initial reactivity studies were performed to evaluate the catalytic potential of the new cations. The half-sandwich **2** catalysed the dimerisation of 1,1-diphenylethylene to 1-methyl-1,3,3-triphenyl-2,3-dihydro-1*H*-indene with 86% conversion after 2 hours at room temperature at 5% loading. Under the same conditions the sandwich complex **1** failed to yield any of the dimerised product. **2** also shows some catalytic activity in the Mukaiyama-aldol addition of methyl trimethylsilyl dimethylketene acetal to benzaldehyde yielding methyl-2,2-dimethyl-3-phenyl-3-trimethylsilyloxypropionate with 14% conversion after 2 hours.

In order to modulate the electronic environment at Sb, targeting an increase in Lewis acidity, we chose to pursue the synthesis of the $[Cp^*SbF]^+$ cation, using an analogous strategy to that employed in the synthesis of **2**. We first developed a route to the previously unreported neutral precursor Cp^*SbF_2 (**3**), which was isolated following the reaction of SbF_3 with one equivalent of Cp*Li. X-ray analysis of the resultant oxygen sensitive yellow crystals demonstrates that **3** is isostructural with Cp^*SbCl_2 in the solid state, comprising molecular units with η^3 Cp* coordination, associated into chains *via* an intermolecular Sb–Cp* interaction (Fig. 33, ESI†).[29]

Reacting **3** with one equivalent of $[(Et_3Si)C_7H_8][B(C_6F_5)_4]$ in toluene at −78 °C results initially in isolation of a yellow oil identified spectroscopically as $[Cp^*SbF][B(C_6F_5)_4]$ (**4**) (Scheme 2).

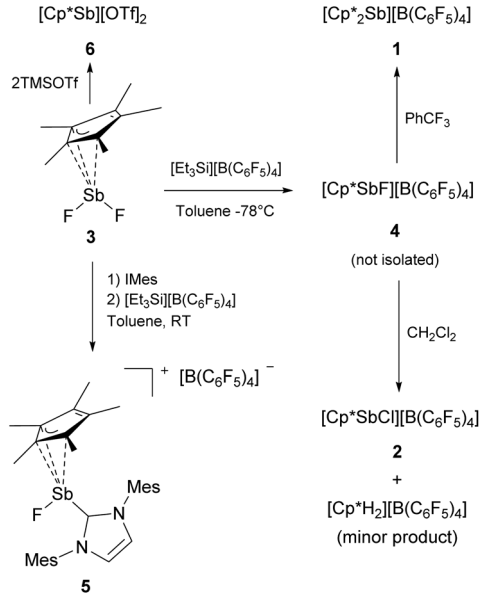

Scheme 2 Synthesis and *in situ* reactivity of **4** and synthesis of **5** and **6**.

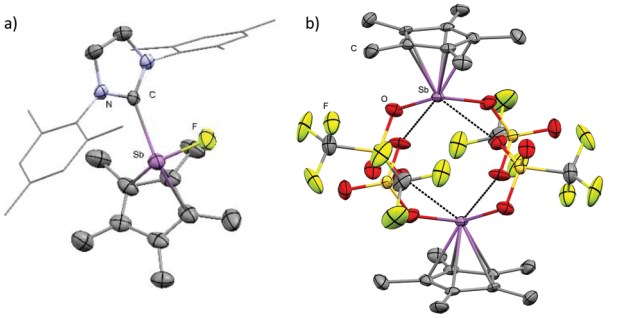

Fig. 3 (a) Solid state structure of the cation in **5**. Ellipsoids are shown at 50% probability. Hydrogen atoms and disordered solvent are omitted for clarity. The hapticity of the Cp* ring is η^3. (b) Solid structure of **6**. Ellipsoids are shown at 50% probability. Intermolecular Sb–O interactions are shown as a dotted line. Hydrogen atoms are omitted for clarity. The hapticity of the Cp* ring is η^5.

However, this species is thermally unstable and all attempts to purify it in the absence of chlorinated solvent resulted in isolation of the sandwich complex **1** (74% by Cp*) and formation of an intractable black solid. When dichloromethane is used in the workup of **4**, a light yellow solid is isolated which was identified as a mixture of **2** and a small amount of $[Cp^*H_2][B(C_6F_5)_4]$ by NMR spectroscopy. Decomposition to $[Cp^*H_2][B(C_6F_5)_4]$ has also been observed for the As analogue $[Cp^*AsF][B(C_6F_5)_4]$[27] and as a product of the reaction between Cp*H and $[Ph_3C][B(C_6F_5)_4]$.[32–34] In no case has the H source been identified. The generation of the chloride derivative **2** is most easily rationalised as the result of a chloride/fluoride exchange between **4** and the dichloromethane solvent. Only a small number of previous studies report fluorodechloroination of dichloromethane at room temperature,[35,36] meriting further investigation of this Swarts type reactivity. A crude sample of **4** was dissolved in $PhCCl_3$, generating $PhCCl_2F$ slowly as identified by ^{19}F NMR spectroscopy (Fig. 17–19, ESI†). No exchange was observed upon addition of $PhCCl_3$ to the decomposition products obtained after workup of **4**, suggesting it is the unstable fluorostibocenium which is responsible.

In order to establish the identity of **4** unambiguously, we sought to trap the reactive Cp^*SbF^+ fragment by forming a stable Lewis base adduct. Addition of the NHC ligand IMes (1,3-dimesitylimidazol-2-ylidene) to **3** followed by addition of $[(Et_3Si)C_7H_8][B(C_6F_5)_4]$ yielded $[Cp^*SbF(IMes)][B(C_6F_5)_4]$ (**5**) on workup. The structure of the cation in **5** shows one IMes ligand co-ordinated to the Cp^*SbF^+ fragment normally, giving a highly distorted trigonal pyramidal Sb centre (Fig. 3a). Crystals of **5** appear thermally stable under a N_2 atmosphere, though they decompose rapidly in air. **5** is a rare example of an NHC complex with a main group metallocene fragment.[37–39]

Attempts to isolate the $[Cp^*Sb]^{2+}$ dication by the treatment of either Cp^*SbCl_2 or **3** with two equivalents of $[(Et_3Si)C_7H_8][B(C_6F_5)_4]$ failed, though recrystallization of the crude products from the latter reaction in CH_2Cl_2 resulted in the isolation of co-crystallised **2**/**4** (Fig. 34, ESI†), giving further proof of the existence of the elusive **4**. However, treatment of Cp^*SbCl_2 with two equivalents of $[Me_3Si][OTf]$ yielded the extremely sensitive pink solid $[Cp^*Sb][OTf]_2$ (**6**).

X-ray structure analysis reveals that the triflate anions are strongly co-coordinated to the Sb centre (mean Sb–O = 2.47 Å). The structure consists of two pseudo-square pyramidal Sb moieties (τ_5 = 0.15) associated *via* a total of four longer intermolecular Sb···OTf contacts (Fig. 3b).[40] The Sb–$Cp^*_{centroid}$ distance (2.092 Å) is contracted in comparison to the other compounds reported here (*cf.* 2.294 Å and 2.142 Å for **1** and **2** respectively), suggestive of an increased positive charge at Sb.

DFT calculations were used to gain further insight into the electronic structures and reactivities of the stibocenium species described above. The geometries of **1**, **2** and **4** were optimised at the M062X/def2SVP level of theory in conjunction with the D3 empirical dispersion correction. Their Lewis acidities were probed using calculated fluoride ion affinities (FIAs). The FIAs (Table 8, ESI†) suggested the Lewis acidity increases in the order $Cp^*_2Sb^+$ (628 kJ mol^{-1}) < Cp^*SbCl^+ (733 kJ mol^{-1}) < Cp^*SbF^+ (741 kJ mol^{-1}). All have higher FIAs than SbF_5 (532 kJ mol^{-1}) when calculated at the same level of theory. When FIAs are calculated with a solvent correction (dichloromethane), the FIAs of these cations retain the same trend but are no longer higher than that of SbF_5. This suggests that absence of any observable Lewis acidic reactivity in **1** could be a consequence of steric hindrance at the Sb centre (Fig. 31, ESI†). In **1**, the LUMO and LUMO+1 are virtually degenerate orbitals of p_y and p_z character respectively. The HOMO is primarily of Cp* π character and the lone pair is pacified to HOMO−2. The primary Sb–Cp* bonding interaction is encompassed in the HOMO−3 (Fig. 37, ESI†). The electronic structures of **2** and **4** are qualitatively equivalent (Fig. 38 and 39, ESI†). The LUMO and LUMO+1 are non-degenerate orbitals of p_y and p_z character respectively. The HOMO−1 incorporates

the Sb–Cp* bonding interaction and the lone pair is pacified to HOMO−4.

Both **2** and **4** are dimeric in the solid state. To probe whether this dimerisation is retained in solution, their structures were modelled in benzyl chloride using a polarizable continuum model, which predicts that the **2** and **4** are mostly monomeric in solution (Fig. 41, ESI†). The mechanism for fluoride/chloride exchange was also probed computationally (Fig. 40, ESI†). In the case of exchange between $PhCCl_3$ and **4**, the most plausible mechanism is initiated by chloride abstraction from $PhCCl_3$ by Cp^*SbF^+, generating a carbocation intermediate (*via* TS1, $\Delta G^{\ddagger} = 18.0$ kcal mol^{-1}), which then abstracts fluoride from Cp*SbFCl (TS2, $\Delta G^{\ddagger} = 6.8$ kcal mol^{-1}). The reaction is exergonic overall ($\Delta G^{\ddagger} = -9.0$ kcal mol^{-1}). Attempts to model exchange between CH_2Cl_2 and Cp^*SbF^+ suggest that this proceeds by a different mechanism which could not be elucidated.

In conclusion, we have synthesised a series of stibocenium cations $Cp^*_{2-n}SbX_n^+$ (X = F, Cl; n = 0, 1) and $Cp^*_{3-n}Sb(OTf)_n$ (n = 1, 2) and investigated the relationship between their structure and reactivity. Replacement of a Cp* ligand with a halide yields significant Lewis acidity. The reactive fluorostibocenium species (Cp^*SbF^+) carries out an unprecedented Swarts type fluorodechloroination under ambient conditions. We are currently further investigating the reactivity of these cations.

Conflicts of interest

There are no conflicts to declare.

Acknowledgements

Funding was provided by the Engineering and Physical Science Research Council (EP/R020418/1), Royal Society of Chemistry (M19-4223) and Nottingham Trent University. The authors wish to acknowledge the Irish Centre for High-End Computing (ICHEC) for the provision of computational facilities and support.

Notes and references

1 L. C. Wilkins and R. L. Melen, *Coord. Chem. Rev.*, 2016, **324**, 123–139.
2 J. Spielmann, F. Buch and S. Harder, *Angew. Chem., Int. Ed.*, 2008, **47**, 9434–9438.
3 T. A. Engesser, M. R. Lichtenthaler, M. Schleep and I. Krossing, *Chem. Soc. Rev.*, 2016, **45**, 789–799.
4 J. Zhu, M. Pérez and D. W. Stephan, *Angew. Chem., Int. Ed.*, 2016, **55**, 8448–8451.
5 C. B. Caputo, L. J. Hounjet, R. Dobrovetsky and D. W. Stephan, *Science*, 2013, **341**, 1374–1377.
6 J. M. Bayne and D. W. Stephan, *Chem. Soc. Rev.*, 2016, **45**, 765–774.
7 B. Pan and F. P. Gabbaï, *J. Am. Chem. Soc.*, 2014, **136**, 9564–9567.
8 M. Yang and F. P. Gabbaï, *Inorg. Chem.*, 2017, **56**, 8644–8650.
9 R. Arias Ugarte, D. Devarajan, R. M. Mushinski and T. W. Hudnall, *Dalton Trans.*, 2016, **45**, 11150–11161.
10 S. Benz, A. I. Poblador-Bahamonde, N. Low-Ders and S. Matile, *Angew. Chem., Int. Ed.*, 2018, **57**, 5408–5412.
11 P. Scilabra, G. Terraneo and G. Resnati, *J. Fluor. Chem.*, 2017, **203**, 62–74.
12 N. L. Kilah, S. Petrie, R. Stranger, J. W. Wielandt, A. C. Willis and S. B. Wild, *Organometallics*, 2007, **26**, 6106–6113.
13 L. Dostál, P. Novák, R. Jambor, A. Růžička, I. Císařová, R. Jirásko and J. Holeček, *Organometallics*, 2007, **26**, 2911–2917.
14 C. J. Carmalt, D. Walsh, A. H. Cowley and N. C. Norman, *Organometallics*, 1997, **16**, 3597–3600.
15 T. J. Kealy and P. L. Pauson, *Nature*, 1951, **168**, 1039–1040.
16 R. C. J. Atkinson, V. C. Gibson and N. J. Long, *Chem. Soc. Rev.*, 2004, **33**, 313–328.
17 N. Dwadnia, J. Roger, N. Pirio, H. Cattey and J. C. Hierso, *Coord. Chem. Rev.*, 2018, **355**, 74–100.
18 P. Štěpnička, *Coord. Chem. Rev.*, 2017, **353**, 223–246.
19 W. E. Geiger, *Coord. Chem. Rev.*, 2013, **257**, 1459–1471.
20 M. A. Beswick, J. S. Palmer and D. S. Wright, *Chem. Soc. Rev.*, 1998, **27**, 225.
21 P. Jutzi and N. Burford, *in Metallocenes: Synthesis Reactivity Applications*, Wiley-VCH Verlag, Weinheim, 1st edn, 1998, pp. 3–51.
22 P. Jutzi and N. Burford, *Chem. Rev.*, 1999, **99**, 969–990.
23 H. Sitzmann, Y. Ehleiter, G. Wolmershäuser, A. Ecker, C. Üffing and H. Schnöckel, *J. Organomet. Chem.*, 1997, **527**, 209–213.
24 A. Kraft, J. Beck and I. Krossing, *Chem. – Eur. J.*, 2011, **17**, 12975–12980.
25 R. J. Wiacek, J. N. Jones, C. L. Macdonald and A. H. Cowley, *Can. J. Chem.*, 2002, **80**, 1518–1523.
26 J. Zhou, L. L. Liu, L. L. Cao and D. W. Stephan, *Chem*, 2018, **4**, 2699–2708.
27 J. Zhou, L. L. Liu, L. L. Cao and D. W. Stephan, *Angew. Chem.*, 2019, **58**, 5407–5412.
28 H. C. Tseng, C. T. Shen, K. Matsumoto, D. N. Shih, Y. H. Liu, S. M. Peng, S. Yamaguchi, Y. F. Lin and C. W. Chiu, *Organometallics*, 2019, **38**(22), 4516–4521.
29 R. A. Bartlett, A. Cowley, P. Jutzi, M. M. Olmstead and H. Stammlerq, *Organometallics*, 1992, **11**, 2837–2840.
30 V. N. Sapunov, K. Kirchner and R. Schmid, *Coord. Chem. Rev.*, 2001, **214**, 143–185.
31 P. Jutzi, T. Wippermann, C. Krüger and H. Kraus, *Angew. Chem., Int. Ed. Engl.*, 1983, **22**, 250–250.
32 M. Otto, D. Scheschkewitz, T. Kato, M. M. Midland, J. B. Lambert and G. Bertrand, *Angew. Chem., Int. Ed.*, 2002, **41**, 2275–2276.
33 J. B. Lambert, L. Lin and V. Rassolov, *Angew. Chem., Int. Ed.*, 2002, **41**, 1429–1431.

34 J. N. Jones, A. H. Cowley and C. L. B. Macdonald, *Chem. Commun.*, 2002, 1520–1521.
35 J. H. Holloway, E. G. Hope, P. J. Townson and R. L. Powell, *J. Fluor. Chem.*, 1996, **76**, 105–107.
36 V. V. Grushin, *Angew. Chem., Int. Ed.*, 1998, **37**, 994–996.
37 C. H. Wang, Y. F. Lin, H. C. Tseng, G. S. Lee, S. M. Peng and C. W. Chiu, *Eur. J. Inorg. Chem.*, 2018, **2018**, 2232–2236.
38 C. Müller, A. Stahlich, L. Wirtz, C. Gretsch, V. Huch and A. Schäfer, *Inorg. Chem.*, 2018, **57**, 8050–8053.
39 C. T. Shen, Y. H. Liu, S. M. Peng and C. W. Chiu, *Angew. Chem., Int. Ed.*, 2013, **52**, 13293–13297.
40 A. W. Addison, T. N. Rao, J. Reedijk, J. Van Rijn and G. C. Verschoor, *J. Chem. Soc., Dalton Trans.*, 1984, 1349–1356.